Proceedings of the 2008 IEEE/ASME
International Conference on Advanced Intelligent Mechatronics
July 2 - 5, 2008, Xi'an, China

Design and Hydrodynamic Modeling of A Lake Surface Cleaning Robot

Zhongli Wang[1,2], Yunhui Liu[1], Hoi Wut Yip[1], Biao Peng[1], Shuyuan Qiao[1], and Shi He[1]

[1]*Department of Mechanical and Automation Engineering*
The Chinese University of Hong Kong
Shatin, NT, Hong Kong, China
yhliu@mae.cuhk.edu.hk

[2]*Department of Computer Science*
Beijing Institute of Technology
Beijing,100081, China
zlwang@mae.cuhk.edu.hk

Abstract **– This paper presents the design and hydrodynamic model of an autonomous robot for cleaning rubbish floating on the surface of a lake. We first address criteria and technical issues in designing such a lake surface cleaning robot (LSCR). A prototype robot with 4 pontoons is further developed. This paper also models hydrodynamics of the prototype robot using the Maneuvering Model Group (MMG) model approach based on a simplified model of three degrees of freedom. The hydrodynamic forces and moments of the pontoons, propulsion and steering forces are derived. Using the hydrodynamic model, we have conducted numerical simulations on viscous resistance of the water, the velocity field and pressure field around the robot.**

Index Terms – Lake Surface Cleaning Robot, Manoeuvring Model Group (MMG), Hydrodynamics

I. INTRODUCTION

There are a large number of lakes or ponds at public parks and gardens. There are also a large number of reservoirs in the world for various purposes. On the surfaces of the lakes, ponds, and reservoirs is floating a lot of rubbish such as dead fish, leaves, small branches, cans, and other small objects. The rubbish is accumulated in particular after rainstorms or strong winds. The floating rubbish certainly affects appearance of lakes and pollutes water when they decay. Therefore, it is important to regularly clean the lake surface and remove the floating rubbish in order to protect cleanness of the water and hence the environment.

Several efforts have been made to development of machines for removal of the floating rubbish on the surface of a lake. In 1992, the Floating Debris Removal Program for the Anacostia and Potomac Rivers was initiated by the local government of the District of Columbia in USA as a pilot project to address debris control problems [1][2]. On market, there are several commercial products such as the TRASHCAT trash skimmer boat developed by the United Marine International (UMI), the trash skimmer boat "ECO 100" developed by Ecomarine, USA. There are also rubbish cleaning boats developed in Changsha, China [11]. However, these commercial products are targeted to applications in big lakes, and hence are not suitable for small lakes like those at public parks. For small lakes, the cleaning task is performed by human workers riding on a small boat. This manual approach is not effective and efficient. Therefore, it is highly demanded to develop an effective, automatic or semi-automatic system for cleaning rubbish floating on the surface of a lake. No such a system is available on market or being developed.

In order to address the needs and provide an innovative solution to cleaning lake surface, this paper proposes to develop an autonomous robot targeted for applications in lakes with small or medium size. The proposed robot can carry out the cleaning task at either autonomous mode or tele-operation mode which allows users to remotely control the robot from offices with real-time haptic force, visual and other feedback. A prototype of such a robot is presented in this paper. The prototype robot uses four pontoons to suspend the weight. The multi-pontoons structure has advantages of generating large internal volume and deck area and having good transverse stability. On the other hand, this structure poses several new technical challenges in hydrodynamic modelling and analysis for its complicated geometry compared to conventional ship design. Since there are limited data and information for designing mu1ti-hull boats, numerical hydrodynamic model and analysis are important for designing the autonomous lake surface cleaning robot.

To model the hydrodynamics of a boat, generally there are two methods proposed , respectively, by Abkowitz [3] and by Mathematical Model Group (MMG) [4]. Both approaches build a mathematical model to describe the hydrodynamic force acting on a boat during manoeuvring and to obtain the hydrodynamic coefficients. In the MMG model, the hydrodynamic force is mainly composed of three components: namely the bare hull, propeller, and rudder force components which are determined by their respective sources. The model considers interactions of the force components. For the simple and clear physical meaning of the coefficients, the MMG model is being widely used for manoeuvring prediction [5]. To analyse the manoeuvring performance of our prototype LSCR, this paper adopts the MMG model.

This paper consists of 5 sections. Section 2 presents design of the lake surface cleaning robot. Section 3 addresses the hydrodynamics model. Simulation results are demonstrated in Section 4. Finally, we conclude this work in Section 5.

II. SYSTEM DESIGN

This section presents the design of the prototype of the lake surface cleaning robot. The prototype robot is targeted to

cleaning floating rubbish at the Weiyuan Lake at The Chinese University of Hong Kong (CUHK)

A. Design Requirements

To fit the rubbish cleaning task in the small lake, several factors and requirements should be taken into account in designing the robot Following are the major design requirements:

- Be able to collect various kinds of rubbish such as dead fish, cans, leaves, small branches and objects, floating on the surface of a lake.
- Be able to move in the small lake autonomously or by tele-operation of human operators.
- The maximum payload should not be smaller than 150kg and the volume of rubbish it can carry is more than 0.6 m^3.
- Be able to avoid collisions with obstacles such as lakeshore of the lake, etc.
- Should be compact in size and light in weight.
- Be able to work continuously for 3-4 hours after fully charged.

The major difficulties in developing the robot are how to cope with the contradictory requirements of reducing weight and size but increasing the payload, to accommodate more rubbish, the requirement of long operation hours with limited power supply, etc.

B. Rubbish Collection Mechanism

Designing the mechanism for collecting the floating rubbish is one of the major issues in the development of the robot. Most of the floating rubbish is small and deformable, and hence it is hard to use a robot manipulator to grasp them. Furthermore, it is inefficient to use a robot manipulator to pick up the floating rubbish one by one. Here, we adopt the conveyor belt mechanism to collect the floating rubbish (Fig. 1). Small baffles are added to the belt so as to move up the rubbish floating on the water surface as the conveyor belt moves. The belt is made from stainless steel with regular meshes to reduce the weight and to allow the water leak. This mechanism is being used in many cleaning boats and its effectiveness has been proven through real applications. The conveyor mechanism has the advantages of being simple in design, easy to control, suitable for collecting different kinds of rubbish, and low in cost.

To select the motor for driving the conveyor belt, it is necessary to estimate the payload. Since the workload of the conveyor belt is fluctuant, we use a redundant power to compensate for this. The torque of the motor is calculated according to the following formula.

$$\tau_{driver} = \tau_{belt} + (I_{wheel} * 4 + I_{rollwheel} * 2 + I_{motor} + I_{gearbox}) a_d ,$$

where a_d is the angular acceleration of the motor, τ_{belt} is the necessary torque for driving the belt, and I_{wheel} , $I_{rollwheel}$, I_{motor} , $I_{gearbox}$ are the inertia moments of all rotational parts. Then $\tau_{motor} = \tau_{driver} / G$, τ_{motor} is the torque output needed to drive the conveyor belt. $\boldsymbol{G}$ is the gear ratio and $G = 100$ in our design. $\tau_{driver} = 40.3596\ N \cdot m$.

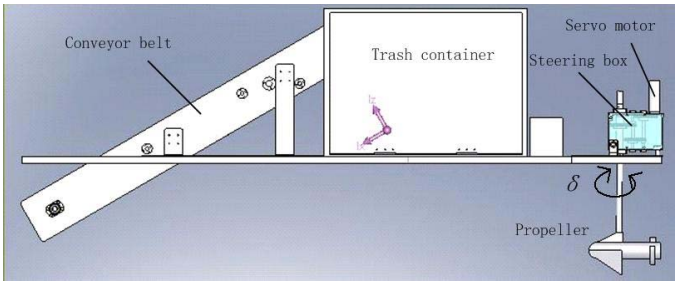

Fig. 1 The change of the gravity centre with full load

C. Driving Mechanism

To freely move on the surface of a lake, the robot needs to have three degrees of freedom. We adopt the drive and steering mechanism to realize the 3 DOF motion. A propeller is used to generate the driving force for controlling the speed of the robot (Fig. 1). By changing the fan speed of the propeller, the magnitude of the driving force generated can be controlled. The direction of the driving force is controlled by a steering mechanism. A brushless DC servo motor is employed to change the orientation angle of propeller, i.e. the thrust direction of the propeller. The angular range of the steering control is between (-90,90) degrees.

D. Sensors

The sensors of the lake surface cleaning robot are categorized according to their functions as follows:

- Sensors for obstacle detection and avoidance: The ultrasonic sensors are being developed for this robot.
- Sensors for localization: Localization is one of the most difficult problems for the robot because it is difficult to install landmarks on water surface and there is no natural landmark for localization. We will integrate the IMU information and GPS to develop a new localization algorithm.
- Sensor for visual information feedback: When tele-operating the robot, it is necessary to view the surrounding environment of the robot. A vision system that enables operators to view the surrounding environment is being developed.

E. Body Design

There are two major technical issues in designing the body of the robot. The first issue is geometric design of the hull. The primary requirement of the hull design is to generate a sufficient force suspending the robot in water. The secondary requirements include reducing hydrodynamic resistance, minimizing the power consumption, and minimizing the size and weight, etc. To simplify the problem, the robot developed by us uses four productive pontoons to suspend the robot. The payload of the four pontoons is 480kg and their weight is 80kg.

How to achieve static balance in water is an important issue in designing the robot. The robot must be able to lie in

water steadily without any inclination in both cases when the rubbish container is empty and when it is full. This presents a big challenge in placing the weights in the robot. First, the robot is made symmetric along the sailing direction. The four pontoons are so placed so that the centre of floating force is located at the symmetric axis. The weights are so placed that the centre of mass of the robot is 5cm away from the centre of floating force in the direction towards the bow of the robot when the rubbish container is empty. When the container contains rubbish, the center of mass will move towards the stern and reaches a location that is 19cm away from the floating force centre when the rubbish contiainer is full (i.e. 190kg). The varying range of the centre of mass is between +5cm and -19cm, which is within the safe range of the robot.

F. Control and Electronics System

Figure 2 shows the block diagram of the LSCR. The mechanical components consist of the conveyor belt, a trash container, a propeller, a steering mechanism, and a body frame. The electronic components include the power supply, the DC motor for driving the conveyor belt, the sensors, the DC motor for controlling the speed of the propeller, the servo motor for steering the direction of the propeller, and the RF module for wireless communication.

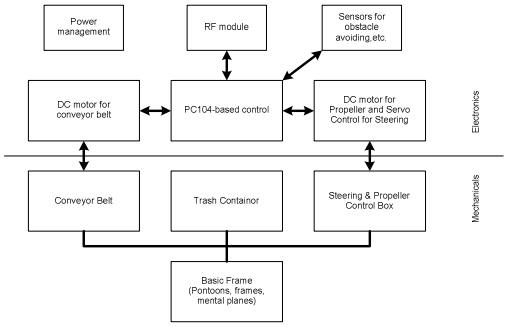

Fig. 2 The block diagram of the LSCR

The electronic components are controlled by a PC104-based control system. All of the electronic peripherals are connected to the PC104 via serial ports. The PC104 turns on or off the DC motor driving the conveyor belt whose speed is fixed. The speed of the DC motor driving the propeller can be controlled by the control system. The control system also controls the steering angle of the propeller. In addition, it also manages the power consumption of the electronic components. When the robot is to run out of power, the control system will send signals to operators and turn off the conveyor belt automatically.

The robot will be able to work at either autonomous mode or tele-operation mode. The tele-operation mode allows users to remotely control the robot from offices with real-time haptic force, visual and other feedback. At the first stage, the tele-operation mode implemented only allows operators standing on the lakeshore to tele-operate the robot via the wireless communication link. The Internet-based teleoperation and autonomous control are being developed.

a) Front view

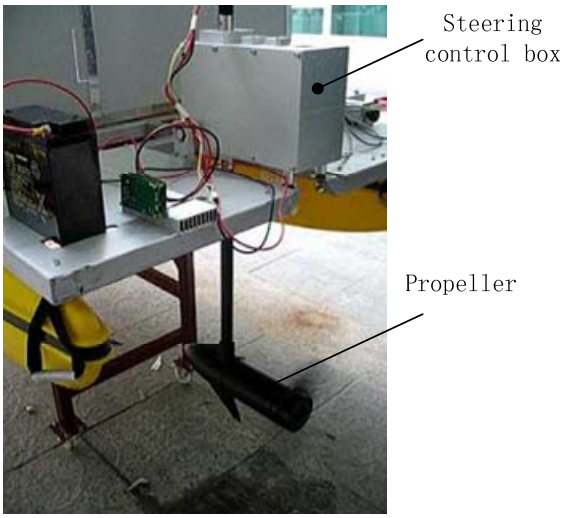

b) Back view

Fig.3 Physical appearance of LSCR

III. HYDRODYNAMIC MODELLING

This section presents the hydrodynamic model of the lake surface cleaning robot. The motion of a robot in water is actually of six degrees of freedom. To simplify the analysis, we assume that the robot moves on the flat surface and neglect other motion. The MMG model approach is used here to derive the hydrodynamic model of the LSCR with three degrees of freedom.

A. The Dynamics

To represent motion of the LSCR, we establish two coordinate frames: namely the inertial frame and the robot frame. The inertial frame is fixed on the earth. The robot frame is fixed on the robot. The origin of the robot frame is located at the centre of mass of the robot when the rubbish container is empty. The z-axis is perpendicular to the water surface and the x-axis is along the symmetric axis of the robot. The third axis is determined from the two axes by the right-hand rule. As shown in Figure 4, the notations used in this paper comply with the SNAME [1950]. The details about frames of ship motion can be referred to references [6] and [7].

In manoeuvring, motion of the LSCR is mainly on horizontal plane, which is referred to surge, sway, and heading, or yaw (rotation about the vertical axis). The

generalized position, velocity, and force vectors are defined in the following. The position-orientation vector of the robot with respect to the inertial frame is

$$\eta = [x \quad y \quad \psi]^T .$$

The linear-angular velocity vector of the robot with respect to the robot body frame is

$$v = [u \quad v \quad r]^T .$$

The position-orientation rate vector $\dot{\eta}$ is related to the velocity vector via:

$$\dot{\eta} = J(\eta)v .$$

where

$$J(\eta) = \begin{bmatrix} \cos\psi & -\sin\psi & 0 \\ \sin\psi & \cos\psi & 0 \\ 0 & 0 & 1 \end{bmatrix},$$

and $r = \dot{\psi}$.

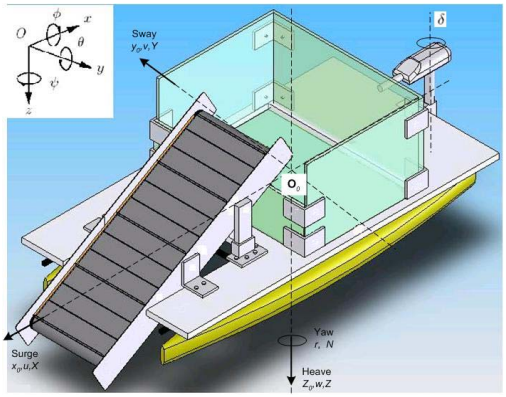

Fig. 4 The notation and sign conventions for ship motion description

The force and moment applied on the robot is defined as the following vector:

$$\tau = [X \quad Y \quad N]^T$$

The force and moment include those generated by different sources and can be separated into components according to their sources:

$$\tau = \tau_{hyd} + \tau_{drv} + \tau_{env} + \tau_{belt}, \tag{1}$$

where, τ_{hyd} is the force and moment generated from motion of the robot in the water, and it includes the inertial hydrodynamic force and the viscous hydrodynamic force. τ_{drv} is the control force generated from the propeller and the steering control. τ_{env} is the force and moment acting on the robot due to the environmental disturbances, e.g., wind, currents and waves. Since we assume that the robot works in calm water, the forces generated by current, waves, and wind can be neglected. τ_{belt} is the water resistance of applied to the conveyor belt, which can be also neglected. Therefore, we have $\tau_{env} = \tau_{belt} = 0$.

Because the robot is bilateral symmetry along the plane *xoz*, then $I_{xy} = I_{yz} = 0$. For the planar motion of the robot, according to the MMG model approach, the dynamics has the following form:

$$\begin{aligned} m(\dot{u} - rv) &= X_I + X_H + X_{PR} \\ m(\dot{v} + ru) &= Y_I + Y_H + Y_{PR} \\ I_{ZZ}\dot{r} &= N_I + N_H + N_{PR} \end{aligned}, \tag{2}$$

where, m is the mass, (X_I, Y_I, N_I) are the forces and moment of the inertial hydrodynamics, (X_H, Y_H, N_H) are the forces and moments of viscous hydrodynamics, (X_{PR}, Y_{PR}, N_{PR}) are the forces and moments of the propeller and steering mechanism. I_{ZZ} is the inertia moment about the z axis.

B. Inertial Force and Momentum of Hulls

Let $\vec{K} = (K_x, K_y)^T$ is the added kinetic energy, and J_{zz} is the added inertia momentum along the *z*-axis, and the added mass matrix is simplified to

$$m = \begin{bmatrix} m_x & 0 & 0 \\ 0 & m_y & m_y\alpha_x \\ 0 & m_y\alpha_x & J_{zz} \end{bmatrix}.$$

Then,

$$\begin{aligned} K_x &= m_x u \\ K_y &= m_y v + m_y \alpha_x r \\ I_z &= m_y \alpha_x v + J_{zz} r \end{aligned}, \tag{3}$$

where α_x are the coordinates of the added mass m_y. And then,

$$\begin{aligned} X_I &= -(\frac{d\vec{K}}{dt})_x = -[m_x\dot{u} - r(m_y v + m_y\alpha_x r)] \\ Y_I &= -(\frac{d\vec{K}}{dt})_y = -[m_y\dot{v} + m_y\alpha_x\dot{r} + m_x ur] \\ N_I &= -(\frac{d\vec{I}_O}{dt})_z = -[(m_y\alpha_x\dot{v} + J_{zz}\dot{r}) + u(m_y v + m_y\alpha_x r) - m_x uv] \end{aligned}. \tag{4}$$

By replacing the items in formula (2) with (4), we have the following dynamic equation:

$$\begin{aligned} (m + m_x)\dot{u} - (mv + m_y v + m_y\alpha_x r)r &= X_H + X_{PR} \\ (m + m_y)\dot{v} + m_y\alpha_x\dot{r} + (m_x + m)ru &= Y_H + Y_{PR} \\ (I_{ZZ} + J_{zz})\dot{r} + (\dot{v} + ur)m_y\alpha_x + (m_y - m_x)uv &= N_H + N_{PR} \end{aligned} \tag{5}$$

C. Viscous Hydrodynamic Force

Several methods are available to calculate the hydrodynamic resistance, such as the wing theory [8][10], the slender-body theory [9], and the linear and nonlinear Taylor expansion. The viscous hydrodynamic forces are made up of a number of different components. This paper considers only the linear part according to linear hydrodynamic derivative coefficient. For simplification, we assume that the viscous fluid just depends on the transient motion status, and is not relative to the historical motion. Then the viscous fluid force and moment can be expressed as a function of current status,

$$\tau_H = f(u; v; r) .$$

Assumed that the robot is in a steady surging motion, with the initial status, $u_0 \neq 0$, $v_0 = r_0 = 0$. Then the linear Taylor expansion can be expressed as following,

$$\begin{aligned} X_H &= X_0(u_0, v_0, r_0) + X_u \Delta u + X_v v + X_r r \\ Y_H &= Y_0(u_0, v_0, r_0) + Y_u \Delta u + Y_v v + Y_r r \\ N_H &= N_0(u_0, v_0, r_0) + N_u \Delta u + N_v v + N_r r \end{aligned} \tag{6}$$

From the geometry symmetry of the robot, we have $Y_u = N_u = 0$ and $X_v = X_r = 0$. Then eq. (6) is simplified to,

$$\begin{aligned} X_H &= X_0(u_0, v_0, r_0) + X_u \Delta u \\ Y_H &= Y_v v + Y_r r \\ N_H &= N_v v + N_r r \end{aligned} \tag{7}$$

D. Driving Force and Moment of the Propulsion and Steering System

The thrust T and torque Q of propeller are dependent on the diameter of propeller (D_p), speed (V_A), density (ρ), viscous coefficient (ν), and acceleration of gravity (g). It can be expressed as

$$T = f(D_p, n, V_A, \rho, \nu, g).$$

Generally, it's difficult to compute the thrust analytically. Regression approach based on database will be adopted to compute the coefficient of thrust and torque.

For the valid thrust calculation of propeller, two effects should be taken into consideration. The first is the wake effect, which makes a difference between the speed of the robot V and the average flow velocity over the axis of the propeller V_a. The wake speed (u_a), is expressed as a fraction of the speed V. Then we have,

$$V_A = V - u_a$$

Let $w = \frac{V - V_a}{V}$, then $V_A = (1 - w)V$.

The other important effect is the thrust deduction due to the interaction between the propeller and the hull. The common practice is to view this increase in resistance as a deduction from the thrust generated by the propeller. This is described by a thrust deduction number t_p,

$$t_p = \frac{T - \Delta T}{T},$$

where, ΔT is the part of T. Then the valid thrust T_a is

$$T_a = (1 - t_p)T \tag{8}$$

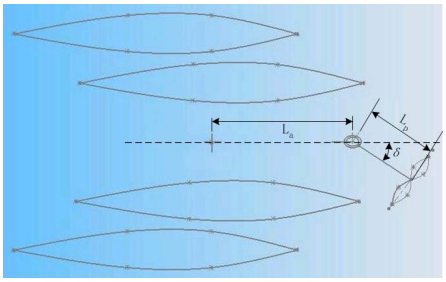

Fig. 5 The location of propeller and thrust

As shown in Figure 5, the main axis of the propeller was located on the symmetry plane *xoz*, the length between the axis and the origin is L_a, the arm length of the propeller is L_p. Then, the force and torque can be expressed as,

$$\begin{aligned} X_{PR} &= T_a \cos\delta \\ Y_{PR} &= T_a \sin\delta \\ N_{PR} &= T_a \cdot L_a \sin\delta \end{aligned} \tag{9}$$

F. Hydrodynamic Model of the Robot

By replacing the correspondent items in eqs. (6) with (8) and (10), we can derive the following hydrodynamic model of the lake surface cleaning robot:

$$\begin{aligned} &(m + m_x)\dot{u} - (mv + m_y v + m_y \alpha_x r)r = X_0(u_0, v_0, r_0) + X_u \Delta u + T_a \cos\delta \\ &(m + m_y)\dot{v} + m_y \alpha_x \dot{r} + (m_x + m)ru = Y_v v + Y_r r + T_a \sin\delta \\ &(I_{ZZ} + J_{zz})\dot{r} + (\dot{v} + ur)m_y \alpha_x + (m_y - m_x)uv = N_v v + N_r r + T_a \cdot L_a \sin\delta \end{aligned} \tag{10}$$

IV. SIMULATION OF VISCOUS HYDRODYNAMIC FORCE

In eq. (1), the environment disturbances and water resistance of the conveyor belt are neglected, and the estimation of the thrust is relatively well-rounded, then we focus more attention to the hydrodynamic force of hulls in this paper. Actually, owing to the different shape of hulls, the estimation of hydrodynamic force is always most difficult part in maneuverability performance analysis. If the hydrodynamic resistance of the robot is R and the thrust is T, then it is obvious that the following condition must be matched for a design of a lake surface cleaning robot:

$$T > R.$$

Based on solving the RANS equations with a finite-analytic method, the three dimensional viscous flows passed LSCR was simulated with CFD. The standard $k - \varepsilon$ turbulence model was applied. And the coupling of velocity and pressure was resolved with the SIMPLE method. Figure 6 shows the computational grid on the surface of the pontoons. Because the robot is symmetric, only half of the robot was used and hence the computational load decreased greatly. In order to increase the precision, a pattern of increment density from outside of the computational domain to hull surfaces was adopted.

The boundary conditions implemented in the computations are as follows.

- Symmetric plane: The symmetry plane is coplanar with the *xoz* plane. There is no flux to the boundary, either convective or diffusive.
- Inlet: All the dependent variables, such as the sailing speed, the parameters of $k - \varepsilon$ turbulence model, should be assigned. There is no pressure boundary condition needed.
- Outlet: Assuming this region is sufficiently long and far downstream for the low speed, the flow may be assumed fully developed. Then the gradients of field variables are ignored.
- Solid wall: The velocity on the solid walls is zero.
- Pressure far field: The fields is far from the hulls, the speed of this field is not affected by the viscous flow.

Figure 7 shows the velocity distribution around the hulls. Figure 8 plots the pressure distribution around the hulls. There are three curves in Figure 9, which respectively represent the

changes of the pressure force, the viscous force and the sum of pressure and viscous force with the Frounde number. Figure 9 shows that pressure force increased proportionally with the increment of Froude number. The results indicate that the viscous force does not change with the increase of the speed. From the simulation results, the pressure force is the major resistance in water. When the sailing speed of the robot is 1m/s, the total resistance force is about 209N. The thrust of the propeller is about 222.3N. The thrust is larger than the resistance, and hence the robot can work properly at this speed.

Fig.6 The computational grid on the surfaces of two pontoons

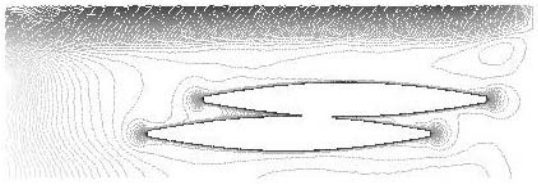

Fig. 7 The velocity distribution around the hulls

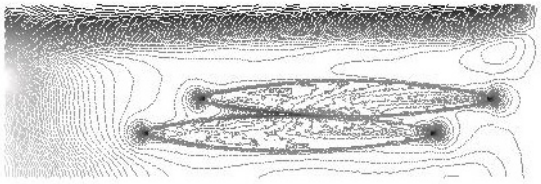

Fig. 8 The pressure distribution around the hulls

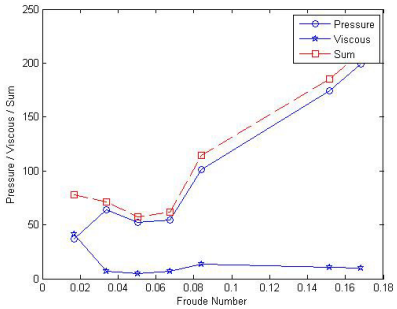

Fig.9 The curve of the viscous resistance and sailing speed

V. CONCLUSION

A lake surface cleaning robot has been developed for cleaning the rubbish floating on surface of a lake in this paper. The design details of the prototype robot are presented. The robot uses four pontoons to suspend the weight and the drive-steering mechanism to realize 3 degrees of freedom motion ion the water surface. The robot can work autonomously or via tele-operation from human operators. Furthermore, we model the hydrodynamics of the lake surface cleaning robot using the MMG modelling approach. The hydrodynamic model provides a basis for motion analysis and controller design of the robot. The hydrodynamic forces are simulated on the basis of the developed model using the CFD-based approach. The simulation results show that the viscous force is independent of the motion speed of the robot, but the pressure force increases with increase of the motion speed. Further development of the robot includes localization algorithm, automatic task planning and navigation in a lake.

ACKNOWLEDGMENT

This work is partially funded by the Estate Management Office (EMO) of The Chinese University of Hong Kong.

REFERENCES

[1] http://www.dredge.com/casestudies/anacostia2.htm
[2] UNITED MARINE INTERNATIONAL(UMI) company, http://www.trashskimmer.com/
[3] M. A. Abkowitz, "Measurement of hydrodynamic characteristics from ship manoeuvering trials by system identification," SNAME Trans. 88 (1980).
[4] E. Kobayashi, H. Kagemoto and Y. Furukawa, "Research on ship manoeuvrability and its application to ship design," In Chapter 2: *mathematical models of manoeuvring motions* (1995), pp. 23–90.
[5] J. B. Petersen, B. Lauridsen, "Prediction of hydrodynamic forces from a database of manoeuvring derivatives," http://www.searchpdf.com/studies/marsim2000/pdf300jbig2/045.pdf
[6] T. Perez, T. I. Fossen, "Kinematic models for manoeuvring and seakeeping of marine vessels," *Modeling, Identification and control*. Vol.28, No.1, 2007, pp.19-30.
[7] Nomenclature for treating the motion of a submerged body through a fluid, SNAME 1950.
[8] K. K. Fedyacvsky, "Application of the results of low aspect ratio wing theory of the solution of some steering problem," *Symposium on the behavior of the ships in a seaway at Wageningen*,1957.
[9] J. N. Newman, "Applications of Slender-Body Theory in Ship Hydrodynamics," *Annual Review of Fluid Mechanics*, Vol. 2, pp. 67-94, 1970.
[10] W. Bollay, "A Non-linear Wing Theory and its Application to Rectangular Wings of Small Aspect Ratio," *ZAMM-Zeitschrift für Angewandte Mathematik und Mechanik*. Vol. 19, Issue 1, pp. 21- 35, Nov 2006.
[11] http://www.qiugou.net.cn/supply/Detail/533424.html